

IV.I High-Temperature Thermochemical

IV.I.1 Solar Hydrogen Generation Research*

Robert Perret (Primary Contact), Yitung Chen, Gottfried Besenbruch, Richard Diver, Alan Weimer, Allan Lewandowski, Eric Miller

UNLV Research Foundation

4550 Maryland Parkway, Box 452036

Las Vegas, NV 89154-2036

Phone: (702) 630-1542; Fax: (702) 413-0094; E-mail: ntsllc@rperret.com

DOE Technology Development Manager: Mark Paster

Phone: (202) 586-2821; Fax: (202) 586-9811; E-mail: Mark.Paster@ee.doe.gov

DOE Project Officer: Doug Hooker

Phone: (303) 275-4780; Fax: (303) 275-4743; E-mail: Doug.Hooker@go.doe.gov

Contract Number: DE-FG36-03GO13062

Subcontractors and Participating Organizations:

General Atomics Corporation, San Diego, CA

The University of Nevada, Las Vegas, Las Vegas, NV

The University of Colorado, Boulder, CO

The University of Hawaii, Honolulu, HI

National Laboratory Collaborators:

Sandia National Laboratories, Albuquerque, NM

The National Renewable Energy Laboratory, Golden, CO

Start Date: October 1, 2004

Projected End Date: December 31, 2005

**Congressionally directed project*

Objectives

- Quantify cost and efficiency of ~3 best solar-powered thermochemical system concepts for the production of hydrogen from water
- Optimize integrated plant design concepts to achieve highest efficiency for minimum hydrogen cost
- Quantify performance and identify operational issues of 3 top thermochemical cycles in integrated loop, bench-scale experiments
 - Scale-up best concept and perform engineering evaluation of a pilot-scale demonstration plant
 - Promote construction and operation of a commercial solar-powered thermochemical hydrogen production plant

Technical Barriers

This project addresses the following technical barriers from the Hydrogen Production section of the Hydrogen,

Fuel Cells and Infrastructure Technologies Program Multi-Year Research, Development and Demonstration Plan:

- AU. High-Temperature Thermochemical Technology
- AV. High-Temperature Robust Materials
- AW. Concentrated Solar Energy Capital Cost
- AX. Coupling Concentrated Solar Energy and Thermochemical Cycles

Technical Targets

This project studies solar-powered high and ultra-high temperature thermochemical production of hydrogen from water. Insights gained will be applied toward the design, demonstration and commercialization of renewable hydrogen production concepts that meet the following DOE 2010 and 2015 hydrogen storage targets:

2010

- Cost at the plant gate: \$6/gge H₂
- Energy Efficiency: 40%

2015

- Cost at the plant gate: \$3/gge H₂
- System Efficiency: 45%

Approach

- Design and implement a quantitative comparative assessment methodology to screen known thermochemical cycles and select the most promising cycles for research
- Perform literature surveys and laboratory experiments to evaluate and design data for the most promising cycles
- Perform feasibility experiments and establish the chemical kinetics of metal sulfates, volatile metal oxides, non-volatile metal oxides and low temperature hybrid cycles like copper chloride
- Design (and test/demonstrate where appropriate) collector/receiver/reactor components for integrated system analysis
- Perform integrated loop bench-scale demonstration experiments for top concepts
- Analyze cost and efficiency metrics for integrated cycle performance
- Develop and implement a demonstration/pilot plant concept design for the top-performing system concept

Accomplishments

- Documented 74 thermochemical cycles previously not screened for performance for a (current) total of ~196 known thermochemical cycles; subsequent analysis showed that these ~196 cycles represented about 180 distinct cycles
- Using automated scoring followed by process thermal efficiency, the initial inventory of 180 cycles was reduced to 5 classes of chemical reactions, each including about 3-4 chemical reactions for which data must be acquired to finalize comparative assessments
- Analyzed receiver/reactor concepts for implementation with various thermochemical cycles with different temperature requirements
 - Identified the solid particle receiver as the most effective advanced power tower concept for most moderate-to-high temperature processes
 - Identified direct solar heating as the most effective concept for ultra-high temperature processes like the volatile metal oxide cycles

- Demonstrated 45% to 75% zinc metal recovery from reduction of ZnO at approximately 1700°C
- Developed a Zn/ZnO process flowsheet and performed “boundary” economic analysis of this thermochemical system
- Analyzed present receiver/reactor design at the NREL High Flux Solar Furnace (HFSF) and initiated improved design studies
- Developed conceptual design of an advanced power tower and heliostat field configuration for ultra-high temperature thermochemical cycles

Future Directions

- Perform necessary studies of the metal sulfate cycles to establish whether:
 - the low temperature reaction occurs spontaneously to form H₂
 - an electrolysis step is required to produce H₂
 - the reaction proceeds in solution to form MSO₄ plus MS, which is the more thermodynamically stable product
- Establish chemical kinetics of:
 - metal oxides
 - volatile metal oxides
 - hybrid copper chloride
- Identify and evaluate other appropriate thermochemical cycles
- Develop and apply dynamic multiphase fluid modeling for the Solid Particle Receiver (SPR):
 - Establish and implement a cold-flow SPR test capability for initial model validation
 - Perform on-sun SPR experiments to validate dynamic thermal simulations
- Apply kinetics information and thermal requirements from laboratory experiments to advanced systems analysis of the top ~14 cycles to identify the ~ 3 most promising cycles
- Improve understanding of the design and economics of a ZnO/Zn cycle solar- thermal water splitting plant
- Complete analysis, design, engineering, fabrication and initial HFSF experimentation with a new fluid-wall cavity reactor for ZnO reduction, including a new secondary concentrator
- Assess performance improvements for advanced tower systems using non-rotationally symmetric secondary concentrators

Introduction

Solar-powered thermochemical water splitting produces hydrogen by using only water, heat from the sun, and chemicals that are completely re-cycled. Hydrogen and oxygen are produced in the process while only water is consumed. Thermochemical water splitting has been shown to be feasible [1, 2, 3, 4, 5]. However, known thermochemical cycles face obstacles that could include extremely high temperature, highly corrosive chemicals, difficult separations of chemicals during sequential cycle steps, multiple reaction steps necessary to close the cycle, or side reactions that poison the recycling process. Many barriers can be overcome, but add

additional costs, inhibit acceptable production rates, or prevent plant designs with acceptable lifetimes. Overcoming these barriers is even more difficult when solar radiation is the driving energy source. Solar radiation is transient, has a relatively low power density [6, 7], and is unacceptable to most large plants because of the difficulty of starting and achieving stable operations. Low power density of solar power also requires large collector areas and efficient concentrators to drive energy-intensive processes.

Promising thermochemical cycles have been identified in several classes of chemical reactions, including metal sulfates, volatile metal oxides, non-

volatile metal oxides and the sulfur-iodine cycle. More work is needed to determine the end-products of intermediate reactions and chemical kinetics, and separation techniques to identify the best competitive cycles for further development. Meanwhile, design studies of reactor concepts integrated with solar receivers will identify performance limits, materials requirements, and cost estimates.

Approach

Assessing the nearly 200 known water splitting cycles has identified cycles unworthy of further evaluation. This qualitative assessment is based on block diagrams of each process that identify the number of reaction steps and reaction temperatures, the physical state of the reactants and products (solid, liquid, vapor), the number of separations, and conceptual description of connections from one step to the next. Sixteen criteria are identified that affect cost, development risk, environmental risk, and sensitivity to power transients. Simultaneously, performance metrics are being established for zinc oxide. Similar metrics will be determined for other attractive cycles like the metal oxides and metal sulfates. All cycles are automatically scored against four solar collector options (trough, standard tower, dish and advanced tower) using software developed for this purpose. About 40 survivors of this screening have been subjected to a detailed evaluation that addresses cycle thermodynamics, estimated performance of solar collector/receiver options, and development of process flow sheets to permit estimates of process efficiency, the primary discriminator for Phase 2 screening. The ~1–3 best cycles will be developed in detail. Demonstration/pilot plant designs will be initiated and recommendations for further work will be provided for concepts that appear competitive.

Results

Thermochemical cycles have been documented in a publicly accessible Solar Hydrogen Generation Research (SHGR) database available at <http://shgr.unlv.edu/>. As new cycles are discovered and analyzed, they will be added to the database. Decision documents are archived for later reference.

Phase 1 Screening: Thermochemical cycles were scored according to 16 criteria designed to select cost-effective processes for hydrogen production. Automated scoring software is described in Section III of Appendix A on the SHGR website. Metrics, including operating temperature criteria (Appendix D on the website) and weighting functions were developed for the four solar power concepts (trough, tower, dish and advanced tower). Most surviving candidates favored the dish (for ultra-high temperature cycles) and the advanced power tower. A score rated each cycle for the appropriate collector. This comparative assessment process was analyzed by Sandia National Laboratories using a Monte Carlo uncertainty analysis that recommended about 50 candidates (Appendix B on the website). Accordingly, the top ~68 scoring cycles were selected for Phase 2. These top scoring cycles can be found on the SHGR website.

Cycles in the database are identified by a process identifier number, or PID #. Table 1 lists 17 of the most efficient cycles from Phase 1, their PID numbers, the chemical reaction steps needed to make hydrogen and close the cycle, the assumed temperature of each distinct reaction step, the calculated cycle thermal efficiency (based on lower heating value of hydrogen), and the scores achieved by each cycle in the automated scoring process. The total scores have different bases depending on the type of solar concept used. These have been normalized to reflect common bases (0-100) in the column labeled Norm Score.

Thermal efficiencies in Table 1 were calculated as part of the Phase 2 evaluation. Table 1 has been sorted according to highest-to-lowest thermal efficiency because thermal efficiency has been identified as the most useful characteristic for lowest cost hydrogen production.

Phase 2 Screening: The 50 cycles selected in Phase I were analyzed in Phase II for energy efficiency. The calculation of thermal efficiency was defined as

All work was done using the higher heating value (HHV), and the final report also includes efficiencies based on the lower heating value (LHV)

Table 1. Phase 1 Scoring Results Sorted by Cycle Thermal Efficiency

PID	Cycle name	Effic. (LHV)	T	Reaction	Total	Norm Score
110	Sodium Manganese-3	50	100	$2\alpha\text{-NaMnO}_2 + \text{H}_2\text{O} = \text{Mn}_2\text{O}_3 + 2\text{NaOH(a)}$	225	43.27
			1560	$2\text{Mn}_2\text{O}_3(\text{l}) = 4\text{MnO}(\text{l}) + \text{O}_2(\text{g})$		
			630	$2\text{MnO}(\text{l}) + 2\text{NaOH}(\text{l}) = 2\alpha\text{-NaMnO}_2 + \text{H}_2(\text{g})$		
106	High temperature electrolysis	49.1	850-2700	$2\text{H}_2\text{O} = 2\text{H}_2(\text{g}) + \text{O}_2(\text{g})$	386	74.23
147	Cadmium Sulfate	46.5	200	$\text{CdO} + \text{SO}_2 + \text{H}_2\text{O} = \text{CdSO}_4 + \text{H}_2$	197	37.88
			1000	$2\text{CdSO}_4 = 2\text{CdO} + 2\text{SO}_2 + \text{O}_2$		
5	Hybrid Cadmium	45.1	1200	$2\text{CdO}(\text{s}) = 2\text{Cd}(\text{g}) + \text{O}_2(\text{g})$	193	37.12
			25	$\text{Cd} + 2\text{H}_2\text{O}(\text{l}) = \text{Cd}(\text{OH})_2 + \text{H}_2(\text{g}) (0.02 \text{ v})$		
			375	$\text{Cd}(\text{OH})_2(\text{g}) = \text{CdO} + \text{H}_2\text{O}(\text{g})$		
6	Zinc-Zinc Oxide	45	2200	$2\text{ZnO}(\text{l}) = 2\text{Zn}(\text{g}) + \text{O}_2(\text{g})$	289	55.58
			900	$\text{Zn} + \text{H}_2\text{O}(\text{g}) = \text{ZnO} + \text{H}_2(\text{g})$		
182	Cadmium Carbonate	44.3	1200	$2\text{CdO} = 2\text{Cd}(\text{g}) + \text{O}_2$	179	34.42
			300	$2\text{CdCO}_3 = 2\text{CO}_2 + 2\text{CdO}$		
			25	$\text{Cd} + \text{CO}_2 + \text{H}_2\text{O} = \text{CdCO}_3 + \text{H}_2$		
2	Nickel-Manganese Ferrite	44	800	$\text{NiMnFe}_4\text{O}_6 + 2\text{H}_2\text{O} = \text{NiMnFe}_4\text{O}_8 + 2\text{H}_2(\text{g})$	261	50.19
			1000	$\text{NiMnFe}_4\text{O}_8 = \text{NiMnFe}_4\text{O}_6 + \text{O}_2(\text{g})$		
194	Zinc-Manganese Ferrite	44	1000	$\text{MnFe}_2\text{O}_4(\text{s}) + 3 \text{ZnO}(\text{s}) + \text{H}_2\text{O}(\text{g}) = \text{Zn}_3\text{MnFe}_2\text{O}_4(\text{s}) + \text{H}_2$	266	51.15
			1200	$2\text{Zn}_3\text{MnFe}_2\text{O}_4(\text{s}) = 2\text{MnFe}_2\text{O}_4(\text{s}) + 6 \text{ZnO}(\text{s}) + \text{O}_2$		
67	Hybrid Sulfur	43.1	850	$2\text{H}_2\text{SO}_4(\text{g}) = 2\text{SO}_2(\text{g}) + 2\text{H}_2\text{O}(\text{g}) + \text{O}_2(\text{g})$	290	55.77
			77	$\text{SO}_2(\text{g}) + 2\text{H}_2\text{O}(\text{l}) = \text{H}_2\text{SO}_4(\text{l}) + \text{H}_2(\text{g})$		
7	Iron oxide	42.3	2200	$2\text{Fe}_3\text{O}_4(\text{l}) = 6\text{FeO}(\text{l}) + \text{O}_2(\text{g})$	298	57.31
			700	$3\text{FeO} + \text{H}_2\text{O}(\text{g}) = \text{Fe}_3\text{O}_4 + \text{H}_2(\text{g})$		
191	Hybrid Copper Chloride	41.6	430	$2 \text{Cu}(\text{s}) + 2 \text{HCl}(\text{g}) = 2 \text{CuCl}(\text{l}) + \text{H}_2$	235	45.19
			75	$4 \text{CuCl}(\text{aq}) = 2 \text{Cu} + 2 \text{CuCl}_2(\text{aq}) (\text{V=})$		
			550	$4\text{CuCl}_2(\text{s}) + 2\text{H}_2\text{O} = 4\text{CuCl}(\text{l}) + 4 \text{HCl} + \text{O}_2$		
149	Barium-Molybdenum Sulfate	39.5	25	$\text{BaMoO}_4 + \text{SO}_2 + \text{H}_2\text{O} = \text{BaSO}_3 + \text{MoO}_3 + \text{H}_2\text{O}$	203	39.04
			1000	$2\text{BaSO}_4 + 2\text{MoO}_3 = 2\text{BaMoO}_4 + 2\text{SO}_2 + \text{O}_2$		
			25	$\text{BaSO}_3 + \text{H}_2\text{O} = \text{BaSO}_4 + \text{H}_2$		
1	Sulfur-Iodine	38.1	850	$2\text{H}_2\text{SO}_4(\text{g}) = 2\text{SO}_2(\text{g}) + 2\text{H}_2\text{O}(\text{g}) + \text{O}_2(\text{g})$	218	41.92
			300	$2\text{HI}(\text{g}) = \text{I}_2(\text{g}) + \text{H}_2(\text{g})$		
			100	$\text{I}_2(\text{a}) + \text{SO}_2(\text{a}) + 2\text{H}_2\text{O} = 2\text{HI}(\text{a}) + \text{H}_2\text{SO}_4(\text{a})$		
193	Multivalent sulfur-3	35.5	850	$2\text{H}_2\text{SO}_4(\text{g}) = 2\text{SO}_2(\text{g}) + 2\text{H}_2\text{O}(\text{g}) + \text{O}_2(\text{g})$	177	34.04
			1570	$2\text{H}_2\text{S}(\text{g}) = \text{S}_2(\text{g}) + 2\text{H}_2(\text{g})$		
			490	$3\text{S}_2(\text{g}) + 4\text{H}_2\text{O}(\text{g}) = 4\text{H}_2\text{S}(\text{g}) + 2\text{SO}_2(\text{g})$		

Table 1. Phase 1 Scoring Results Sorted by Cycle Thermal Efficiency

PID	Cycle name	Effic. (LHV)	T	Reaction	Total	Norm Score
			150	$3\text{SO}_2(\text{g}) + 2\text{H}_2\text{O}(\text{l}) = 2\text{H}_2\text{SO}_4(\text{l}) + \text{S}$		
131	Manganese Sulfate	35.4	1100	$2\text{MnSO}_4(\text{s}) = 2\text{MnO}(\text{s}) + 2\text{SO}_2 + \text{O}_2$	234	45
			290	$\text{MnO}(\text{s}) + \text{SO}_2 + \text{H}_2\text{O} = \text{MnSO}_4(\text{s}) + \text{H}_2$		
72	Calcium-Iron Bromide-2	33.8	600	$2\text{Br}_2(\text{g}) + 2\text{CaO} = 2\text{CaBr}_2 + \text{O}_2(\text{g})$	208	40
			600	$3\text{FeBr}_2 + 4\text{H}_2\text{O}(\text{g}) = \text{Fe}_3\text{O}_4 + 6\text{HBr}(\text{g}) + \text{H}_2(\text{g})$		
			750	$\text{CaBr}_2(\text{l}) + \text{H}_2\text{O}(\text{g}) = \text{CaO} + 2\text{HBr}(\text{g})$		
			300	$\text{Fe}_3\text{O}_4 + 8\text{HBr}(\text{g}) = \text{Br}_2(\text{g}) + 3\text{FeBr}_2 + 4\text{H}_2\text{O}(\text{g})$		
70	Hybrid Sulfur-Bromine	33.4	850	$2\text{H}_2\text{SO}_4(\text{g}) = 2\text{SO}_2(\text{g}) + 2\text{H}_2\text{O}(\text{g}) + \text{O}_2(\text{g})$	229	44.04
			77	$2\text{HBr}(\text{ia}) = \text{Br}_2 + \text{H}_2(\text{g})$		
			77	$\text{Br}_2(\text{g}) + \text{SO}_2(\text{a}) + 2\text{H}_2\text{O} = 2\text{HBr}(\text{a}) + \text{H}_2\text{SO}_4(\text{a})$		

of hydrogen. Here, $\Delta H_{25^\circ\text{C}}(\text{H}_2\text{O})$ is the higher heating value for water (the heat of formation of liquid water at 25 C), and Q_{hot} is the total high temperature heat required from the solar heat source, W_s is the net amount of shaft work and pumping power. The next term in the denominator is the electrical energy cost for a hybrid cycle: ΔG_T is the thermodynamic energy of the electrolytic reaction under standard conditions, the $RT\ln()$ term corrects for the solution concentrations, and the nFE_{OV} term corresponds to the overvoltage needed (0.2 V for no membrane separator, or 0.4 V for a hybrid with a membrane separator). The factor of 0.5 represents 50% efficient generation of electricity from other sources to perform the electrolysis.

$$\eta = \frac{-\Delta H_{25^\circ\text{C}}(\text{H}_2\text{O})}{Q_{\text{hot}} + \frac{W_s + \Delta G_T^\circ + RT \ln \left(\frac{\prod a_p^{n_p}}{\prod a_r^{n_r}} \right) + nFE_{\text{OV}}}{0.5}}$$

Each reaction was evaluated using the program HSC Chemistry 5.0, to verify that the reported reaction (a) had a negative (or at least not a large positive) free energy of reaction, and (b) the reported high temperature reaction gave products in the lowest energy state. Unless a reaction with a positive free

energy was amenable to electrolysis, the cycle was assigned zero efficiency, and the analysis ceased. The second factor (b) is significant, because we found reactions which had a negative free energy of reaction—thereby satisfying criteria a), but the desired products were not the lowest energy state. For instance, in the manganese sulfate cycle, the high temperature step purported to make pure $\text{MnO}(\text{s})$. The thermodynamic analysis showed that $\text{MnO}(\text{s})$ was only about 10%–20% of the total Mn species produced at 1150°C, and significant amounts of MnO_2 and Mn_2O_3 were also produced, thus reducing the amount of O_2 produced in the reaction. This oxidation of Mn to higher valences, and the reduction of O_2 produced, has the effect of reducing the efficiency of the cycle by 5-10 fold. The evaluation of these other products, using HSC, is a critical part of assessing the cycles. The application of criteria (b) is not as straightforward for low temperature reactions. At low temperatures, where chemical reactions are slower, it is possible to form the less energetically favored products if the reaction forming the thermodynamically favored products cannot be readily realized due to high activation energy.

Flow sheets and energy balances were created for each of the cycles which had reasonable thermodynamics. For each step in the flowsheet, reasonable assumptions were made for separation

methods, heat exchangers, etc. The initial flowsheet was done, presuming the reactions as written went to completion.

Cycles which had high efficiencies (>40% using HHV) were then further assessed by looking at issues like criteria (b) above for MnO at 1150°C. The thermodynamic efficiency was then corrected for such an equilibrium distribution of products, and the lower efficiency was calculated. The efficiency calculations resulted in a consolidated ranking of cycles (Table 2) that reflects the top 14 thermochemical cycles. These 14 cycles had an efficiency >40% based on the higher heating value. The high temperature electrolysis (HTE) process that ranks very high among the top 15 cycles is omitted

because this is a direct electrolysis reaction and not a thermochemical reaction. (HTE is being studied under the Nuclear Hydrogen Initiative. HTE performance will ultimately be compared with the thermochemical cycles to assure completeness.) The 14 top thermochemical cycles were placed into 5 classes due to chemical similarities. Almost all of these cycles are 2 or 3 step cycles. We cannot at this point confidently distinguish between cycles within a class, or decide which class is "better."

The sulfate cycles are composed of two steps:

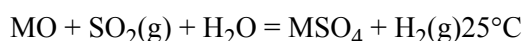


Table 2. Chemical Classes and Cycles Selected for Further Study

PID #	Cycle class and name	kJ input per mole H ₂	MJ input per kg H ₂	Efficiency (lhv) %	Efficiency (hhv) %
	Metal sulfates				
147	Cadmium sulfate	520	260	46.5	55
149	Barium Molybdenum-sulfate	608	304	39.7	47
131	Manganese sulfate	681	340	35.5	42
	Volatile metal oxides				
5	Hybrid cadmium	539	270	44.8	53
182	Cadmium carbonate	550	275	44	52
6	Zinc oxide	537	269	45.0	53.2
	Metal oxides				
2	Nickel-Manganese Ferrite	550	275	44	52
194	Zinc-Manganese Ferrite	550	275	44	52
7	Iron Oxide	572	286	42	50
110	Sodium Manganese-3	484	242	50	59.1
	Sulfuric acid cycles				
67	Hybrid sulfur	560	280	43.1	51
1	Sulfur-iodine	635	318	38.1	45
193	Multivalent sulfur	681	340	35.5	42
	Other interesting cycles				
191	Hybrid copper chloride-2	583	292	41.5	49

The three cycles here have $M(+2)$ cations, (Cd, Ba, Mn) in the basic cycle. PID 149 has a third step, to exchange the sulfate with molybdate, to give a lower decomposition temperature compared to the direct decomposition of $BaSO_4$. There is an open question for all three cycles as to whether:

- the low temperature reaction occurs spontaneously to form H_2 ;
- an electrolysis step is required to produce H_2 ; or
- the reaction proceeds in solution to form MSO_4 plus MS which is the more thermodynamically stable product.

The volatile metal cycles all create $M(g)$ at the high temperature step. The $M(g)$ is condensed, and added to water to regenerate MO and H_2 . In the cadmium cycles, adding Cd(s) to water does not form H_2 spontaneously, so PID 5 requires an electrolysis step, whereas in PID 182, CO_2 is added to make $CdCO_3$ and drive the H_2 evolution reaction.

In the metal oxide cycles, a mixed oxide is exposed to water at low temperatures, to add oxygen to the metal lattice (thereby oxidizing Mn or Fe) and evolving H_2 . At high temperatures, the extra oxide forms O_2 , returning the metal to the lower valence state.

In the sulfuric acid cycles, PID 67 and PID 1 have been very well studied in the past, and the efficiency values were taken from previous work. PID 193 is a 4-step process requiring a much higher temperature to decompose H_2S . There is a formal similarity between the sulfate cycles above, and these sulfuric acid cycles. In the sulfate cycles, the MO is added to make MSO_4 which is decomposed at higher temperatures to make MO, SO_2 and O_2 , whereas PIDs 1 and 67 take H_2SO_4 to the high temperatures to make the analogous H_2O , SO_2 and O_2 . Formally, MO and H_2O distinguish these two classes, and the rest of the cycle is chemically the same. In the "other interesting cycles" category, the only striking feature is the low "high temperature" compared to the other cycles, which makes these more amenable to trough and standard tower solar devices.

The cycles selected to be studied in Phase 3, feasibility, analyses are highlighted in bold in both Tables 1 and 2. Cadmium cycles are not presently being pursued experimentally due to their high

toxicity. However, inquiries are underway to industrial cadmium processors to find out if there are cheap and effective containment strategies for this otherwise interesting cycle. The CuCl cycle is under investigation at the Argonne National Laboratory and the sulfur cycles are being pursued by the Nuclear Hydrogen Initiative. PID 7, Iron Oxide, is one of several ferrite cycles being investigated by this project and so is not called out separately. Finally, Multivalent Sulfur is not being pursued presently, primarily on the grounds that it is somewhat similar to the Sulfur-Iodine cycle. However, its advantage over Sulfur-Iodine is that it does not involve iodine, simplifying some aspects of cycle closure. One disadvantage is that its high temperature step is at much higher temperature than that for Sulfur-Iodine.

Receiver/Reactor Architectures: Various receiver/reactor concepts were evaluated for cycles with the temperatures generally encountered among apparently favored thermochemical processes. The recommended solar architectures and receiver concepts are listed in Table 3. No cycles compatible with parabolic trough use, based on operating temperature needs, were found. Because of the relative simplicity and high temperatures required, the ferrite cycles are suitable for integration with parabolic dishes and possibly with an advanced power tower. Only the Sodium Carbonate-Iodate (PID 196) and perhaps the Argonne National Laboratory Low-Temperature Copper Chloride cycle (PID 191) are suitable for conventional molten-nitrate-salt power towers. The rest require an advanced power tower or a highly concentrating dish to provide the thermal energy to the cycle.

After an extensive screening process, 17 thermochemical cycles from 8 cycle classes were identified that can potentially produce low-cost solar thermochemical hydrogen from water. Thirteen cycles chosen in Phase 2 screening form a subset of 17 cycles. Because of temperature requirements, none of the cycles were found suitable for parabolic troughs. Two cycles might be integrated with conventional molten nitrate salt power towers if temperature requirements of less than $650^\circ C$ can be attained. Because molten nitrate salt power tower technology is well developed and salt heat exchanger/reactors are expected to be straightforward, these cycles are attractive from a

Table 3. Recommended Receivers for the Top Thermochemical Cycles

PID	Cycle Name	Cycle Class	Temp, °C	Solar Architecture	Recommended Receiver	Alternative receiver
2	NiFeMn Ferrite	Ferrite	1800	Dish	Rotating Disk Reactor	Reactive solid particle
7	Iron Oxide	Ferrite	2100	Dish	Rotating Disk Reactor	Reactive solid particle
194	Zn Ferrite	Ferrite	1800	Dish	Rotating Disk Reactor	Reactive solid particle
191	ANL Copper chloride	Chloride	700	Conv. PT Advanced PT	Molten Nitrate Salt	Solid Particle
67	Hybrid Sulfur	Sulfuric acid	850	Advanced PT	Solid Particle	Volumetric Air
1	Sulfur Iodine	Sulfuric acid	900	Advanced PT	Solid Particle	Volumetric Air
5	Cadmium Oxide	Volatile Metal Oxide	1600	Advanced PT	Fluid wall reactor	Centrifugal Reactor
182	Cadmium carbonate	Volatile Metal Oxide	1600	Advanced PT	Fluid wall reactor	Centrifugal Reactor
196	Sodium Carbonate- Iodate	Carbonate	650	Conv. PT	Molten Nitrate Salt	Volumetric Air
131	Manganese sulfate	Sulfate	1500	Advanced PT	Unknown	Solid Particle (Zircon)
147	Cadmium sulfate	Sulfate	1150	Advanced PT	Solid Particle (Zircon)	Volumetric Air
149	Barium molybdenum sulfate	Sulfate	1400	Advanced PT	Unknown	Solid Particle (Zircon)
72	UT-3	Calcium bromide	750	Advanced PT	Solid Particle	Volumetric Air
106	Hi Temp (Steam) Electrolysis	Electrolysis	850	Advanced PT	Solid Particle	Volumetric Air
6	Zinc Oxide	Volatile Metal Oxide	1800	Advanced PT	Fluid Wall	Centrifugal Reactor
110	Sodium Manganese-3	Metal Oxide	1600	Advanced PT	Solid Particle (Zircon)	Unknown
193	Multivalent Sulfur	Sulfuric Acid	1600	Advanced PT	Solid Particle (Zircon)	Unknown

solar integration perspective. All of the other cycles will require solar receiver development. Only the relatively simple Ferrite cycles were determined suitable for parabolic dishes and a new Rotating Disk Reactor concept was invented to simultaneously address the requirements of parabolic dishes and the Ferrite cycles. Most of the attractive thermochemical cycles require an advanced power tower.

For most of the thermochemical cycles, the solid particle receiver is recommended. The solid particle receiver is conceptually simple, does not use hazardous material, and incorporates low-cost thermal energy storage. Under previous development in the 1980s, solid particles were identified for temperatures up to 1200°C. The volumetric receiver is a possible alternative to the

solid particle receiver for temperatures up to about 1000°C but inefficiencies associated with the return air and thermal storage approaches will need to be addressed. For the high-temperature volatile metal Cadmium Oxide cycles, the receiver concepts currently under development for the related Zinc Oxide cycle are recommended. All of the cycles will require further investigation to define the interface between the solar heat and the thermochemical reaction(s). More details of the reactor/receiver selection study can be found in Appendix E on the website.

Zn/ZnO Feasibility Studies: The SHGR Project is exploring a promising class of thermochemical water-splitting cycles known collectively as the “metal-oxide cycles.” While the number of steps in metal oxide cycles varies, all have a common high-temperature step. This is the thermal reduction of a high valence metal oxide to either a lower valence metal oxide or the base metal. Depending on the cycle, temperatures required for these thermal reductions range from 1700 K to 3000 K. In subsequent steps, H₂ is liberated from water and the original high valence metal oxide is restored. The net reaction is always the splitting of water into its constituent hydrogen and oxygen parts.

Two of the metal oxide cycles are of particular interest: Zn/ZnO and MnO/Mn₂O₃. The advantages of these cycles lie in their relatively small numbers of process steps, and the large amounts of information reported on them in the literature. The Zn/ZnO cycle has been the nearly exclusive subject of work performed to date. Advantages of the Zn/ZnO process are its relatively low dissociation step temperature, simple gas/solid separations, and low number of steps. Its main disadvantage is the thermodynamic tendency of Zn(g) and O₂(g) to recombine during cooling of the dissociation reaction products. Prevention of this may require an inefficient rapid cooling of the products, unless research identifies a way to hinder recombination reaction kinetics.

The results of work performed to date are summarized here. For details of the apparatus and experimental results, see Appendix F on the website.

Feasibility experiments were conducted to demonstrate that ZnO can be thermally reduced at low residence times (<1.5 s) and moderately high temperatures (1700-2000°C) with minimal re-oxidation during cooling. Experiments were conducted in the Weimer Group Transport Tube reactor at the University of Colorado. The reactor was a graphite aerosol flow tube heated by a graphite resistance element capable of attaining temperatures as high as 2400°C. The experiments examined temperature conditions from 1700 to 2000°C and reaction times ranging between 1.0 and 1.7 seconds. Collected particles were analyzed using x-ray powder diffraction and fixed oxygen determination using a LECO instrument, as well as transmission electron microscopy (TEM). Products of the experiments included heavier ZnO collected by gravity in the collection vessel, High Efficiency Particulate Air filter material that was Zn metal, and thermophoretically deposited Zn on the walls of the cooling zone of the reactor. Mass balance indicated conversion rate of ZnO to Zn ranging from 45% to 75%.

Reaction kinetics studies are continuing but have been unsuccessful so far due to problems with particle size and the detection of leaks in the experimental apparatus that prevented an accurate determination of residence time in the reaction zone. Additionally, carbothermal reduction of ZnO by CO could introduce artificially high conversion rates and must be explored to assure uncorrupted data. A carbon-free reactor is in development, consisting of Al₂O₃ ceramic material that can sustain operations between 1600 and 1700°C for this purpose.

Design Improvements of the High Flux Solar Furnace at NREL: The National Renewable Energy Laboratory (NREL) is preparing for on-sun experiments of the Zn/ZnO cycle using NREL's High Flux Solar Furnace (HFSF). This facility was used earlier in an earlier project to investigate high temperature methane splitting for hydrogen production without the emission of CO₂.

\Ray-tracing codes and fluid dynamic simulations were applied to the existing design to establish a baseline for comparison of improved design performance. In general, it is believed that converting the original design to a cavity-type

receiver will provide significant improvements by eliminating much of the radiation losses encountered with the earlier design. A design tradeoff of such a change is that the cavity aperture must be small, requiring highly concentrated solar power at the aperture. This is not believed to be a significant obstacle. Design tradeoffs are proceeding as reactor diameter and cavity wall reflectivity effects are analyzed, using integrated model studies of dynamic performance and radiation environments in the cavity. Details of the HFSF design effort are provided in Appendix G on the website.

Advanced Power Tower and Heliostat Field Conceptual Design: NREL is studying advanced concepts to provide exceptionally high temperature environments required for ultra-high temperature thermochemical processes, like volatile metal oxide cycles. Two concentrating solar power technologies have the potential to deliver high concentration levels. The first is dish technology, where sufficient peak and average concentrations have been demonstrated in existing systems. The limitations with dish technology are the relatively small unit size ($\sim 100\text{--}150\text{ kW}_{\text{th}}$) and the distributed nature of the hardware requiring a large number of units to achieve significant plant size. The second, and preferred, technology is a central receiver. However, typical central receivers have not been designed for high enough concentration levels. Thus, the plant will need to be an advanced tower configuration for ultra-high temperature thermochemical cycles. The initial assumptions are that average concentrations of at least 2000 suns (200 W/cm^2) will be needed to drive reactions at temperatures to 2200°C , heliostat field designs will be fundamentally different than for lower temperature applications (e.g. Solar Two), heliostats will need to be smaller and packed more tightly to achieve required flux levels and a secondary concentrator will be needed to achieve required flux levels. NREL commissioned a general systems analysis of advanced tower configurations with the following findings:

- The highest possible concentrations can only be achieved with an axially symmetric circular field surrounding a central tower with a Compound Parabolic Concentrator (CPC) looking downward.

- In the above configuration, the achievable concentration increases asymptotically towards the ideal limit as the CPC acceptance angle, θ_c , is reduced and the tower height increases.
- Although there is no well-defined optimum configuration, 80% of the ideal limit can be achieved in this configuration with a tower height to field diameter ratio of about 1.0.
- As one tilts the CPC view cone towards the north and away from straight down (look out angle, $\gamma > 0$)
 - the intercepted area for heliostats becomes an ellipse of increasing area and eccentricity.
 - the maximum achievable geometric concentration decreases rapidly. This result is independent of scale.
- If the intercept area for heliostats is held constant, the corresponding tower height requirement decreases gradually.
- Obliquity effects (cosine losses) are not prohibitively large in a circularly symmetric surround field geometry, mainly because tower heights are comparable to the field dimensions.
- Effects of blocking and shading and ground cover constraints have not yet been calculated in detail, but could be expected to be less in a surround field geometry than in a north field configuration.
- Furthermore, as noted above, our approach guarantees that the calculated limit already includes the first-order correction for the effects of blocking and shading losses.

Stark conclusions from this study are that a circular surround field of heliostats provides highest concentrations but requires a tall tower configuration. If tower height is limited for any reasons, a north field of heliostats is second best, but peak achievable concentration is reduced by about 33%. Design concepts with north fields and multiple secondary concentrators have been developed and analyzed. Details of this study and its preliminary findings can be found in Appendix G.

Summary

Assumption-driven assessments of thermochemical hydrogen production by the sulfur-

iodine cycle and the zinc oxide cycle were found to indicate that a solar-powered water-splitting hydrogen production concept could be competitive with other processes, at least for some reasonable scenarios. Phase 1 screening has been demonstrated to be sufficiently insensitive to subjective weighting factors to warrant this approach to reducing the inventory of thermochemical cycles for detailed analysis. Phase 2 screening has identified about 14 potentially competitive thermochemical cycles in ~ 5 chemical reaction classes. Inadequate laboratory data exist for further confident comparative evaluation of these cycles. Laboratory work is under way to develop the necessary data.

Collector/receiver concepts have been studied for all of the potentially competitive thermochemical cycles found in Phase 2 screening. A primary concept has been recommended for all cycles and an alternative concept has been recommended for most.

Reduction of ~45% to ~75% particulate ZnO feedstock to metallic Zn has demonstrated the feasibility of this process, warranting continued development of performance metrics and reaction kinetics of this cycle in an operating mode that is insensitive to power fluctuations. Experimental difficulties due to reactor leaks and the possibility of carbothermal reduction of ZnO have so far prevented completion of the reaction kinetics studies, but remediation experiments are under way. Advanced receiver/reactor design efforts continue to define an improved concept for ZnO reduction experiments with NREL's High Flux Solar Furnace. Advanced power tower and heliostat field concepts are being developed and analyzed to support ultra-high temperature thermochemical cycle plant concepts.

References

1. J.E. Funk and R.M. Reinstrom, "System Study of Hydrogen Generation by Thermal Energy," Allison Division, General Motors Rept. EID 3714, Vol. II, Suppl. A, 3.1–3.25 (1964).
2. J.E. Funk and R.M. Reinstrom, "Energy Requirements in the Production of Hydrogen from Water," I&EC Process Design and Development, Vol. 5 (1966) 336.
3. T.N. Veziroglu and F. Barbir, "Hydrogen Energy Technologies," Emerging Technology Series, United Nations Industrial Development Organization, Vienna (1998).
4. A. Steinfeld, "Solar hydrogen production via a two-step water-splitting thermochemical cycle based on Zn-ZnO redox reactions," *International Journal of Hydrogen Energy* 27 (2002) 611– 619.
5. L. C. Brown, G. E. Besenbruch, R. D. Lentsch, K. R. Schultz, J. F. Funk, P. S. Pickard, A. C. Marshall, and S. K. Showalter, "High Efficiency Generation of Hydrogen Fuels using Nuclear Power, Final technical report for the period August 1, 1999 through September 30, 2002", GA-A24285, General Atomics Document issued June 2003.
6. L.G. Radosovich, C.W. Pretzel, E.H. Carrell, and C.E. Tyner, "An Assessment of Solar Central Receiver Systems for Fuels and Chemical Applications," SAND86-8019, Sandia National Laboratories, Albuquerque, NM (1986).
7. C.W. Pretzel, and J.E. Funk, "The Developmental Status of Solar Thermo-chemical Hydrogen Production," SAND86-8056, Sandia National Laboratories, Albuquerque, NM (1987).
8. E.L. Miller, R.E. Rocheleau, and X.M. Deng, *International Journal of Hydrogen Energy*, 28(6), 615-623 (2003), included in the "Attachment 1".
9. X.-D. Xiang,, *Annual Reviews of Materials Science* 29, 149-171 (1999).